

Effect of Inclination Angle and Size of Heated Surface on Pool Boiling CHF

Soo Hyung YANG, Won Pil BAEK, and Soon Heung CHANG

Department of Nuclear Engineering
Korea Advanced Institute of Science and Technology
373-1 Kusong-dong, Yusong-gu, Taejeon, Korea 305-701

ABSTRACT

Pool boiling critical heat flux (CHF) have been investigated using plate type test sections with different widths (3 cm & 4 cm) and lengths (10 cm, 15 cm & 20 cm) under various inclination angles. As the inclination angle increases from 0° (horizontally facing downward plate) to 30°, CHF sharply increases. After that angle, CHF gradually increases with the increase of the inclination angle. There must be a transition angle between 0° and 30°, at which the CHF increase rate remarkably changes. According to the comparison of present and previous experiments, the transition angle may be affected by heater size and increase with the increase of heater size. The size effect of heated surface on CHF is noticeable in the L15 & L20 series and W4 series; however, it seems to be difficult to find the size effect in L10 series and W3 series.

1. INTRODUCTION

The CHF, at which efficient nucleate boiling and inefficient transition/film boiling from the viewpoint of heat transfer are divide, has been considered as one of most important heat transfer characteristic for several decades. For this reason, considerable experimental works and analytical investigations have been performed to identify CHF conditions and underlying CHF mechanism, and to develop mechanistic CHF models. Specially pool boiling CHF condition on an infinite horizontal upward surface is well known compared to other boiling situations and several mechanistic models, i.e. hydrodynamic instability model [1, 2, 3] or macrolayer dryout model [4], have been suggested. These models have been continuously modified with the progress in understanding the physical mechanisms leading to the CHF.

Recently, somewhat unusual condition, to which the application of these general CHF models is limited, are appeared and highlighted with respect to practical applications, i.e. the CHF on a downward-facing plate or curved surface, storage tank carrying hazardous fluids during external fire and microelectronic chips in electrical industry. In this regard, a few ex-

perimental works with water [5~12] and cryogenics [13~20] have been performed following in the footsteps of the industry's request.

However, the understanding levels on the CHF behavior with the inclination angle and the CHF occurrence mechanism, and the phenomenological information related to the bubble behavior at an inclined plate fall behind. In addition, it is ambiguous to describe size effect on the CHF due to the absence of systematic investigation. To clarify and investigate the effect of inclination angle and the size of heated surface on CHF, a series of CHF experiments with plate type test sections have been performed in KAIST. This paper presents the experimental results performed with six different heated surfaces under various inclination angles.

2. EXPERIMENTS

2.1 Experimental Apparatus

The experimental loop, as shown in Fig. 1, has been constructed to identify the CHF behaviors for overall inclination angles at atmospheric pressure. The main parts of experimental loop are a test pool & test section, a power supply system and a data acquisition system. CHF experiments have been conducted in the test pool (600×600×900 mm), which was made up of Type-304 stainless steel except for the front and back parts for the visual observation and recording of the boiling behavior at the heated surface. In the present experiments, demineralized water is used as a working fluid and heated to nearly saturation condition using preheater prior to every experiment. Three Type-T (Copper-Constantan) thermocouples have been used to measure the pool temperature.

Various kinds of test sections have been used to investigate the effect of the width and the length of heated surface on CHF and their dimensions are shown in Table 1. Test sections are made up of Type 304 stainless steel and the upper region of test sections is insulated by high temperature resistant epoxy, as shown in Fig. 2. The epoxy is used for sealing the heated surface and to diminish heat loss from the backside of the test section. Five Type K (Chromel-Alumel) thermocouples, which are used to measure the temperature of heated surface, are embedded at the boundary between heated surface and high temperature resistant epoxy. A copper electrode is welded to each end of stainless steel plate to transfer the electric power from a 40V/5000A DC power supply system connected to it. The inclination angle of the test section

was provided by fastening the test section to the electrode positions installed at the side parts of the test pool.

The voltages and ampere from the thermocouples and test section are directly measured by data acquisition system, which is consisted of a HP Series 300 Workstation, HP 3852A data acquisition/control Unit and IBM PC/486. The heat flux of the test section is directly calculated using the voltage and ampere from the test section. Experimental errors involved in the temperature measurement were estimated to be $\pm 1.6^{\circ}\text{C}$ and $\pm 1.5^{\circ}\text{C}$ for Type-K and Type-T thermocouples, respectively.

CHF is generally defined by the abrupt temperature increase of the heated surface in the case of heat flux controlled system. Unfortunately, if the trip system is not shutdown as soon as possible after the occurrence of CHF, considerable damage of the test section can occur and its break off is sometimes possible. Therefore, the CHF detection criterion is very important for the protection of the test section as well as the exact occurrence detection of CHF. In present experiment, the CHF condition was practically defined as the condition that the resistance of the test section suddenly increased, as shown in Fig. 3. At the occurrence of the CHF, the electrical resistance also sharply increases in the experiment of Golobic & Bergles [21]. Figure 3 shows the appropriateness of this criterion: the electrical resistance change of the test section always occurs prior to the stiff temperature increase of the test section due to the delay time of the thermocouples.

2.2 Experimental Results

Experimental results for all test sections are shown in Table 2 and Fig. 4, respectively. In Fig. 4, the CHF predictions for an infinite horizontally facing upward plate and an inclined plate are also shown.

CHF at Horizontally Facing Upward Plate (180°)

In the case of horizontally facing upward plate, several researchers have performed CHF experiments with different geometries. In addition, Zuber *et al.* [1] and Lienhard & Dhir [2] have suggested hydrodynamic instability models for the prediction of pool boiling CHF. Some of the CHF data at horizontally facing upward plate and the CHF predicted by Zuber *et al.* and Lienhard & Dhir's correlation are shown in Fig. 5. Based on the experimental CHF data, Sada-

sivan *et al.* have suggested the lower and upper bound of pool boiling CHF at horizontally facing upward plate and those values are also shown in Fig. 5.

As shown in Fig. 5, the CHF data at the horizontally facing upward plate are somewhat higher than those predicted by the hydrodynamic instability model. This seems to be the effect of small size of heated surface used in each experiment. For the application of the hydrodynamic instability model, the size of heated surface should be larger than the size limitation (~ 8 cm for saturated water) [3]. However, most of the experiments have been conducted with small-size test sections compared to this size limitation. Therefore, as the large bubble is detached from the heated surface, the water surrounding the heated surface instantaneously and easily rushes to heated surface, even at the center position of heated surface, compared to large heated surface. This phenomenon may also affect the boiling behavior at the heated surface. Through easy water ingress and instantaneous water flow convection to the heated surface, the higher CHF is possible in small heated surface.

In present experiment, the width is smaller than the size limitation (~ 8 cm), therefore, the CHF values at horizontally facing upward plate are higher than those predicted by the hydrodynamic instability model.

Effect of Inclination Angle on CHF

CHF generally increases with the increase of the inclination angle and this behavior is similar to other's previous works, as shown in Fig. 4. However, CHF values and behavior at the facing downward plates identified in the present experiment shows somewhat higher and stiff changes with inclination angle compared to those predicted by El-Genk *et al.* [7, 8] and Vishnev *et al.*'s [15] correlation, respectively. This would be due to different experimental method, material property and geometry of the test section. Among them, the geometry difference would be the main cause of higher CHF and different CHF behavior: 50.8 mm disk (the diameter of surround material is 80 mm) for El-Genk *et al.*'s experiment and 10.4×96 mm for Vishnev *et al.*'s experiment. Considering the characteristic length (width or diameter) and Taylor instability wavelength for the working fluid used in experiments, the characteristic lengths are about $1.86 \lambda_{TD}$ ($2.94 \lambda_{TD}$ in the case of the surround material) and $3.15 \lambda_{TD}$ for El-Genk *et al.*'s and Vishnev *et al.*'s experiment, respectively. In the other hand, the characteristic lengths, i.e. width, of the present experiment are only 1.1 and $1.47 \lambda_{TD}$, which are smaller than other's experiments

(Details are shown in Table 3). These small characteristic lengths have affected the bubble behavior, i.e. easy escape of bubbles generated at the heated surface through lateral direction, and induce somewhat higher CHF value at the same inclination angle. In addition, slight deviation from the horizontally facing downward induces stiff CHF increase rate due to the small characteristic lengths. Additional experiments have been performed using a test section with 6-cm ($2.2 \lambda_{TD}$) width, which is relevant to characteristic lengths used in El-Genk *et al.*'s experiment. According to the experiments, CHF seems to approach the prediction values by El-Genk *et al.* and Vishnev *et al.*'s correlation.

In the case of W3 series and W4L10, the CHF of 30° is somewhat higher than that of 60° . This can be explained by higher detachment frequency of coalesced bubble and easy bubble escape through lateral side. However, in the case of W4L15 and W4L20, CHF linearly increases for overall inclination angles, as shown in Fig. 4 and 6.

Size Effect of Heated Surface on the CHF

The width effects of heated surface for overall inclination angles are shown in Fig. 6. As shown in this figure, it is difficult to evaluate the width effect in L10 series, even at horizontally facing downward position. In the other hand, the width effect on the CHF can be clearly identified in L15 series and L20 series. Related to the length effect on the CHF, its identification is possible only for the W4 series, as shown in Fig. 7. Similar to the L10 series, it is somewhat obscure to define the length effect in W3 series. Difficulty in detecting the width and length effect in L10 series and W3 series can be explained by bubble escape path: bubble easily escape from the heated surface due to short length in L10 series and short width in W3 series. However, as the width of heated surface further increases to 6 cm, CHF values for W6L10 (vertical position: 90°) and W6L15 (60°) decrease to about 900 kW/m^2 , which is about 70 % of CHF predicted by Zuber *et al.*'s correlation. Considering this experimental result, the width effect is clearly identified although the length of the heated surface is comparatively small, as L10 series.

Comparison with Previous Experiment

For the comparison of the present experiment, previous experiments with helium and water are minutely investigated. First of all, the characteristic sizes are converted into non-dimensional number considering Taylor instability wavelength of the working fluid used in ex-

periments. Considering Taylor instability wavelength, the sizes of heated surface and non-heating surface are re-calculated, as shown in Table 4: most of experiments have non-heating surface which surrounds the heated area.

In the case of the experiments with helium, non-dimensional sizes of the heated surface are comparatively larger compared to the present experiment. Therefore, stiff increasing behavior of the CHF with inclination angle is not appeared and CHF values are considerably smaller than present experimental results, till vertical position. However, at the horizontally facing upward position, the CHF is very similar in spite of difference of heated surface size. In addition, the CHF decreases with the increase of the size of the heated surface for overall inclination angles except for the Nishio *et al.*'s [18] experimental result, as shown in Fig. 8 (a). This behavior may result from longer residence time with the increase of the heated surface's size.

In the case of experiment with water, similar behaviors have been identified: increasing CHF with the increase of inclination angle and decreasing CHF with the increase of heater size. In addition, stiff increasing behavior of the CHF with inclination angle is clearly identified in the experiment with small test section: present experiment, Ohama *et al.* [6], Sakashita *et al.*'s experiment [10] and author's previous experiment [11, 12]. The stiff increasing behavior of CHF is also identified in El-genk *et al.*'s experiment. However, the increasing rate of the CHF seems to be somewhat decreased, as shown in Fig. 8 (b). In addition, the CHF values of the present experiment are similar to those of experiment with small size, i.e. Sakashita *et al.* and Ohama *et al.*'s experiment.

Transition Angle Behavior

As referred, the increase rate of CHF considerably changes at certain inclination angle, which is termed as transition angle (θ_{tr}). To identify the behavior of the transition angle, experimental results with different size test section have been examined in detail, as shown in Fig. 9. As shown in Fig. 9, CHF sharply increases with slight deviation from the horizontally facing downward position in the case of the experiments using small plate less than $1.47 \lambda_{T,d}$. The transition angle seems to be located below 10° in the experiments using small plate, according to author's previous work [11, 12], Ohama *et al.* [6] and Sakashita *et al.*'s [10] experimental results. In the author's previous work and present experiment, CHF increase rate with inclination angle considerably decreases after the transition angle: in the other hand, CHF still sharply in-

crease after the transition angle in Ohama *et al.*'s result. The transition angle can be identified in the experiments with somewhat large plate: El-Genk *et al.* [7, 8], Lyon [14] and Iwamoto *et al.*'s [18] experiments. However, CHF increase rate below the transition angle gradually decreases with the increase of the heater size. Considering the speculation lines shown in Fig. 9, the transition angle seems to be located at near 10° in the experiments performed by Lyon and El-Genk *et al.* and can be found at near 15° for Iwamoto *et al.*'s experiment. Based on the above investigation, transition angle may be affected by the size of the heated surface.

3. CONCLUSIONS

An experimental study has been performed to investigate the effects of the heated surface inclination angle and size on the pool-boiling CHF of near-saturated water under atmospheric pressure. Important findings are summarized as follows:

1. At horizontally facing upward plates, measured CHF values are higher than those predicted by the conventional pool boiling CHF correlation: Zuber *et al.* and Lienhard *et al.*'s correlation. The higher CHF values may result from the effects of the easy water ingress to the heated surface and convective flow due to the small size of the heated surface.
2. CHF generally increases with the increase of inclination angle (from horizontally facing downward position to horizontally facing upward position). Two distinct regions have been identified based on the CHF increase rate, i) sharply increasing region till 30° , ii) gradual increasing region after 30° . This induced by the difference of major boiling phenomena with the inclination angle. Peculiar point has been identified in present experiment: i.e. the CHF for 30° inclined plate is larger than that for 60° inclined plate, except for W4L15 & W4L20. This behavior may result from the easy bubble escape from the heated surface due to the small heater size.
3. In the point of the CHF increase rate, there should be a transition angle, at which the CHF increase rate considerably changes. The transition angle seems to be around 10° in the author's previous experiment and seems to be located between 0° and 30° in present experiment. Considering present experiments and previous works, the transition angle must be affected by and may increase with the increase of the characteristic size of heated surface.

4. In the case of W4 series and L15 & L20 series, CHF decreases with the increase of the length and the width of heated surface, respectively. In the other hand, it is difficult to identify the effect of the length and width in W3 series and L10 series. This behavior may result from the easy bubble escape due to the small heater size: the bubbles generated at the heated surface easily escape from the heated surface due to short length in L10 series and short width in W3 series.

Nomenclature

q_{chf}	critical heat flux,	kW/m ²
$q_{chf, Zuber}$	critical heat flux predicted by Zuber correlation	kW/m ²
$\lambda_{T,d}$	Taylor wavelength scale, $=2\pi(3\sigma/g\Delta\rho)^{0.5}$,	m
θ	inclination angle (0° for a horizontal downward-facing plate, 90° for a vertical plate, and 180° for a horizontal upward-facing plate)	
θ_{tr}	transition angle,	degree

References

1. N. Zuber, Hydrodynamic aspects of boiling heat transfer, AEC Report No. AECU-4439, 1959.
2. J.H. Lienhard, V.K. Dhir and D.M. Rihard, Peak pool boiling heat-flux measurements on finite horizontal flat plates, *ASME J. Heat Transfer* **95**, 477-482, 1973.
3. Hewitt, G.F. (1982), *Chapter 6.4 Burnout*, in *Handbook of Multiphase System*, Vol. 1, 6.66-6.141, Hemisphere Publishing Corporation, Washington, D.C., 1982.
4. Y. Haramura and Y. Katto, A new hydrodynamic model of critical heat flux, applicable widely to both pool and forced convective boiling on submerged bodies in saturated liquids, *Int. J. Heat Mass Transfer* **26**, 389-399, 1983.
5. S. Ishigai, K. Inoue, Z. Kiwaki and T. Inai, Boiling heat transfer from a flat surface facing downward, *Int. Dev. in Heat Trans.*, 224-229, 1961.
6. T. Ohama and K. Miyazaki, Influence of inclination on downfacing burnout heat flux in water pool, *J. Nuclear Science and Technology* **23**(12), 1104-1106, 1986.
7. Z. Guo and M.S. El-Genk, An experimental study of saturated pool boiling from downward facing and inclined surfaces, *Int. J. Heat and Mass Transfer* **35**(9), 2109-2117, 1992.
8. M.S. El-Genk and Z. Guo, Transient boiling from inclined and downward-facing surfaces in a saturated pool, *Int. J. Refrig.* **16**(6), 414-422, 1993.
9. V.S. Granovskii, A.A. Sulatskii and S.M. Shmelev, The crisis of nucleate boiling on a horizontal surface facing downward, *High Temp.* **32**(1), 78-80, 1994.
10. H. Sakashita, H. Yasuda and T. Kumada, Studies on pool boiling heat transfer (modification of correlation of macrolayer thickness and measurements of macrolayer thickness at low heat fluxes), *Heat Transfer-Japan. Res.* **25**(8), 522-536, 1996.

11. S. H. Yang, W. P. Baek and S. H. Chang, "Pool-Boiling Critical Heat Flux on Small Plate: Effects of Surface Orientation and Size," *Proc. Of the Korean Nuclear Society Spring Meeting*, Cheju, May 30~June 1, 337-342, 1996.
12. S.H. Yang, W.P. Baek and S.H. Chang, Pool-boiling critical heat flux of water on small plate: effects of surface orientation and size, *Int. Comm. Heat Mass Transfer* **24**(8), 1093-1102, 1997.
13. P.M. Githinji and R.H. Sabersky, Some effects of the orientation of the heating surface in nucleate boiling, *ASME J. Heat Transfer* **85**(4), 379, 1963.
14. D.N. Lyon, Boiling heat transfer and peak nucleate boiling fluxes in saturated liquid helium between the λ and critical temperatures, *Adv. in Cryog. Eng.* **19**, 371-379, 1964.
15. R.P. Anderson, L. Bova, The Role of downfacing burnout in post-accident heat removal, *Trans. Am. Nucl. Soc.* **14**, 294, 1971.
16. I.P. Vishnev, I.A. Filatov, Ya.G. Vinokur, V.V. Corokhov and G.G. Svalov, Study of heat transfer in boiling of helium on surfaces with various orientations, *Heat Transfer-Soviet Res.* **8**(4), 104-108, 1976.
17. B. Beduz, R.G. Scurlock and A.J. Sousa, Angular dependence of boiling heat transfer mechanisms in liquid nitrogen, *Adv. in Cryog. Eng.* **33**, 363-370, 1988.
18. S. Nishio and G.R. Chandratilleke, Steady-state pool boiling heat transfer to saturated liquid helium at atmospheric pressure, *JSME Int. J. Series II* **32**(4), 639-645, 1989.
19. A. Iwamoto, T. Mito, K. Takahata, N. Yanagi and J. Yamamoto, Dependence of heat transfer from a wide copper plate to liquid helium on heat transfer surface orientation and treatment, *Cryogenics* **36**, 139-143, 1996.
20. J.Y. Chang and S.M. You, Heater orientation effects on pool boiling of micro-porous-enhanced surfaces in saturated FC-72, *ASME J. of Heat Transfer* **118**, 937-943, 1996.
21. Iztok Golobic and A.E. Bergles, Effects of heater-side factors on the saturated pool boiling critical heat flux, *Experimental Thermal and Fluid Science* **15**, 43-51, 1997.

Table 1. Test Matrix for Experiment (unit: mm)

Width	Length	100	150	200	
30		W3L10	W3L15	W3L20	W3 Series
40		W4L10	W4L15	W4L20	W4 Series
		L10 Series	L15 Series	L20 Series	

Table 2. Experimental Results (CHF: kW/m²)

Inclination Angle (°)	W3L10	W3L15	W3L20	W4L10	W4L15	W4L20
0	783	667	792	759	531	626
30	1156	1186	1215	1241	1088	1097
60	1129	1189	1145	1166	1109	1098
90	1196	1275	1196	1210	1159	1120
120	1371	1335	1303	1320	1133	1210
150	1340	1311	1315	1268	1281	1259
180	1501	1251	1427	1341	1371	1364

Table 3. Detail Information

	Working Fluid	Geometry & Material of Test Section [mm]	Size of Test Section based on $\lambda_{T,D}$		Method
Guo & El-Genk [6]	Water	Disk Type D = 50.8 [80×80; surround material] Copper	1.86 $\lambda_{T,D}$ [2.94 $\lambda_{T,D}$]		Quenching
Vishnev <i>et al.</i> [15]	He	Plate Type 10.4×96×0.063 Stainless steel	3.15 $\lambda_{T,D}$	28.9 $\lambda_{T,D}$	Steady Heating
Present	Water	Plate Type W = 30, 40 L = 100, 150, 200 Stainless Steel	W = 1.1, 1.47 $\lambda_{T,D}$	L = 3.67, 5.50, 7.33 $\lambda_{T,D}$	Steady Heating

Table 4. Heater Size and Geometry

Author	Geometry of Test Section (mm)		Non-dimensional Size Considering $\lambda_{T,D}$	
	Heated Surface	Surrounding Material	Heated Surface	Surrounding Material
Ohama <i>et al.</i> [6]	Disk : 29.5	Disk : 200	1.08	7.33
El-Genk <i>et al.</i> [7,8]	Disk : 50.8	Plate : 80 × 80	1.86	
Sakashita <i>et al.</i> [10]	Disk : 15	Present; no information	0.55	-
Yang <i>et al.</i> [11,12]	Plate : 20 & 25 × 200	No	0.733 & 0.92 × 7.33	-
Present Experiment	Plate : 30& 40 × 100, 150 & 200	No	1.10 & 1.47 × 3.67, 5.50 & 7.33	
Lyon [14]	Disk : 9.91	Disk : 28.702	2.91	8.44
Vishnev <i>et al.</i> [16]	Plate : 10.4 × 96	No information	3.03 × 28.24	-
Nishio <i>et al.</i> [18]	Disk : 20	Present; no information	5.88	-
Iwamoto <i>et al.</i> [19]	Plate : 18 × 76	Plate : 38 × 90	5.29×22.35	11.17 × 26.47

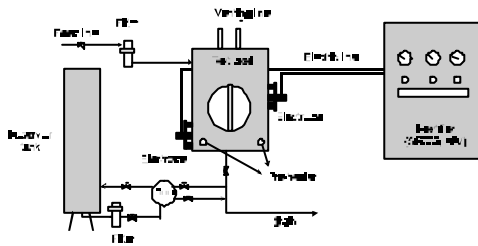


Fig. 1 Schematic Diagram of the Pool Boiling Experimental Loops

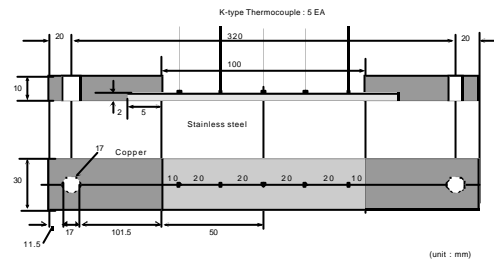
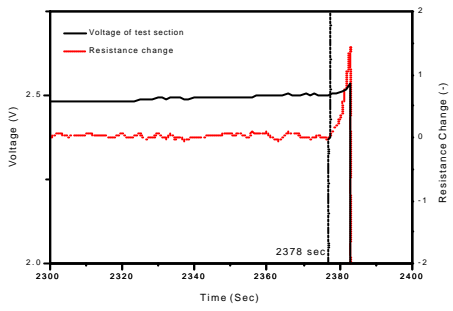
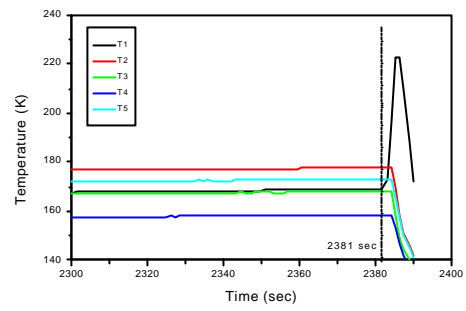


Fig. 2 Schematics of the Test Sections (W3L10 case, unit: mm)



(a) Voltage and Resistance Change Behavior of the Heated Surface



(b) Temperature Behavior of the Heated Surface

Fig. 3 Physical Properties Behavior at CHF

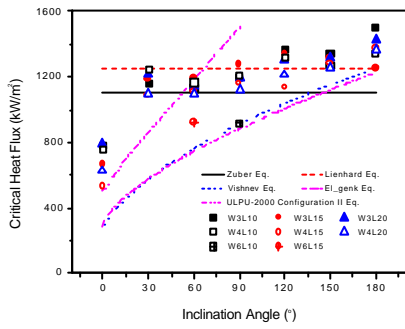


Fig. 4 Overall Behavior of the CHF

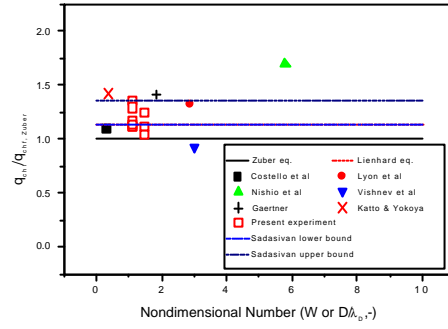


Fig. 5 CHF at Horizontally Facing Upward Plates

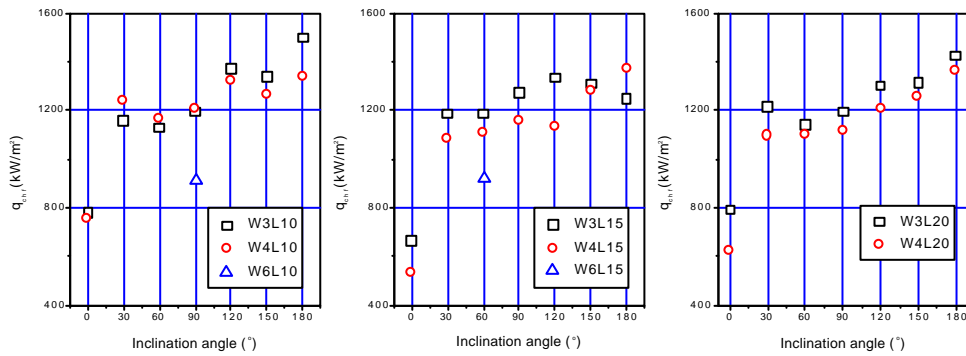


Fig. 6 Width Effect of Heated Surface on CHF

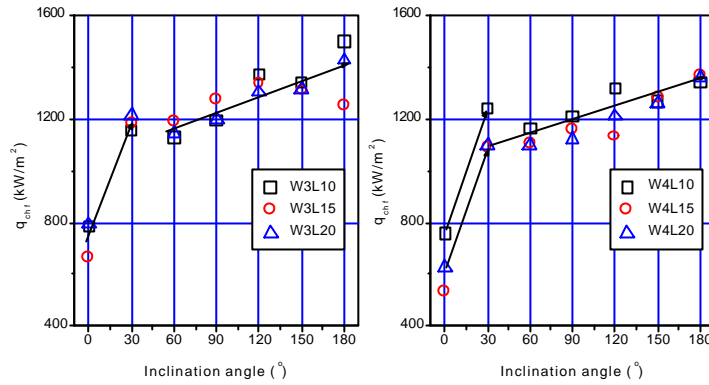
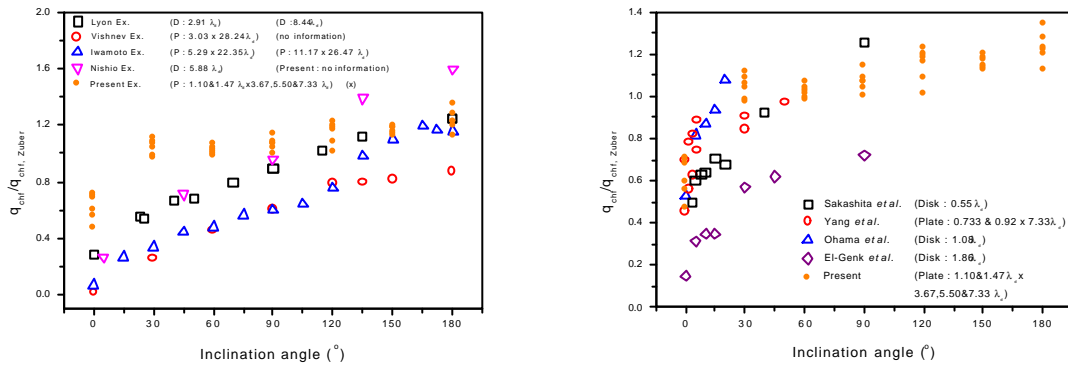


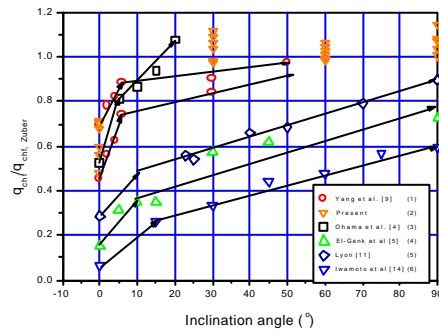
Fig. 7 Length Effect of Heated Surface on CHF



(a) Experimental Results in Helium Pool

(b) Experimental Results in Water Pool

Fig. 8 Comparison of Present Experimental Results with Previous Works



- (1) Plate: $0.733 \times 0.92 \times 7.33 \lambda_{T,d}$, (2) Plate: $0.733 \times 1.47 \times 3.67, 5.50 \times 7.33 \lambda_{T,d}$, (3) Disk: $1.08 \lambda_{T,d}$,
 (4) Disk: $1.86 \lambda_{T,d}$, (5) Disk: $2.91 \lambda_{T,d}$, (6) Plate: $5.29 \times 22.35 \lambda_{T,d}$

Fig. 9 Transition Angle Behavior with Heated Surface Size